Analytical and Bioanalytical Chemistry (2022) 414:5493–5505
https://doi.org/10.1007/s00216-022-03955-2

RESEARCH PAPER

Gallic acid-coated silver nanoparticles as perspective drug nanocarriers: bioanalytical study

Katarína Nemčeková[1] · Veronika Svitková[1] · Jozef Sochr[1] · Pavol Gemeiner[2] · Ján Labuda[1]

Received: 26 November 2021 / Revised: 14 January 2022 / Accepted: 1 February 2022 / Published online: 16 March 2022

Abstract

The ability of silver nanoparticles (AgNPs) to be used as drug nanocarriers has helped rapidly to invent novel strategies to treat diseases, such as cancer. The nanoparticles may offer a valuable tool to novel pH-sensitive drug delivery systems in the present scenario because of their undergoing mechanisms associated with the regulated dissolution, aggregation, and generation of oxygen radicals as well. These processes could be monitored by electrochemical (bio)sensors that are less money and time-consuming compared to other analytical approaches, however, with comparable analytical performance. In this paper, synthesized and microscopically characterized gallic acid-coated AgNPs (GA-AgNPs) are investigated using spectral and electrochemical methods. To investigate the Ag^+ release, a 21-day ageing experiment is performed spectrophotometrically, finding that the peak maximum of GA-AgNPs spectra diminished by 24.5%. The highest Ag^+ content was electrochemically determined in the supernatant solution after centrifugation (6.97 μmol·L^{-1}), while no significant concentration of silver ions in solution after redispersion was observed (1.26 μmol·L^{-1}). The interaction experiment indicates a stabilization of GA-AgNPs in the presence of long-chain dsDNA as well as a mutual electrostatic interaction with DNA sugar-phosphate backbone. This interaction mechanism is confirmed by FTIR analysis, showing a shift (1049 to 1061 cm^{-1} and 913 to 964 cm^{-1}) specific to DNA phosphate bands. Finally, doxorubicin-loaded GA-AgNPs are monitored for the specific drug release in the physiological and more reactive weakly acidic microenvironment. Hereby, electrochemical (bio)sensing of GA-AgNPs undergoing mechanisms shows a huge potential to be used for monitoring of drug delivery systems at cancer therapy.

Keywords Silver nanoparticles · Aggregation · Silver ion release · DNA interaction · Electrochemical biosensor · Drug delivery system

Introduction

Silver nanoparticles (AgNPs) as very promising and attractive nanomaterials have been of interest especially in biomedical applications since they showed antimicrobial activity. These properties come out from their ability to produce reactive oxygen species (ROS) acting towards biomolecules and against pathogenic microbes [1]. Thus, under ambient condition, oxygen molecules are adsorbed on the AgNPs surface, therefore, oxidize the surface to form silver ions, while the oxygen molecules are spontaneously reduced to ROS, such as superoxide and hydroxyl radicals. The released silver ions then bind to negatively charged phospholipid-based cell membranes, thus, affect the membrane stability, either physically or chemically via an oxidation mechanism leading to cell death. Moreover, the intracellular silver ions may bind to thiol groups of proteins and enzymes located on the cellular surface which can cause membrane destabilization and the

Published in the topical collection featuring *Promising Early-Career (Bio)Analytical Researchers* with guest editors Antje J. Baeumner, María C. Moreno-Bondi, Sabine Szunerits, and Qiuquan Wang.

✉ Katarína Nemčeková
katarina.nemcekova@stuba.sk

[1] Institute of Analytical Chemistry, Faculty of Chemical and Food Technology, Slovak University of Technology in Bratislava, Radlinského 9, 81237 Bratislava, Slovakia

[2] Department of Graphic Arts Technology and Applied Photochemistry, Faculty of Chemical and Food Technology, Slovak University of Technology in Bratislava, Radlinského 9, 81237 Bratislava, Slovakia

inhibition of their activity. The biomolecule-AgNPs interactions strongly depend on the surface properties of AgNPs and thus influence the AgNPs uptake into cells. That is why the surface modification is a key factor in biomedical use [2].

Both the ROS generation and the release of silver ions have been shown as critical steps in the AgNPs-induced effect against biomolecules. Till now, many papers have discussed the potentially toxic influence of AgNPs on biomolecules of different organisms from small microbial cells [3, 4] to human cells [5–7]. However, the term "toxicity" may be interpreted in both positive and negative ways depending on, whether the goal represents a benefit or a potential hazard. It is necessary to disinfect/sterilize surfaces and areas, e.g., in medical facilities, especially during the COVID-19 outbreak. Hereby, the antimicrobial activity/toxicity of AgNPs has a huge positive impact on human health. On the other hand, when the same (nano)material undergoes an unintended or undesired mechanism including the spontaneous release of silver ions Ag^+ and the production of ROS, then such toxicity can be defined as a negative outcome. The processes related to the AgNPs can be effectively used in targeted drug delivery systems as drug nanocarriers, especially as nanocarriers of chemotherapeutics for cancer treatment and therapy. Upon targeting the drug to a tumor cell, AgNPs release the drug due to the physical or chemical changes in tumor cell microenvironment which leads to their destabilization; thus, the oxidation of silver to Ag^+ with the spontaneous ROS formation occurs. These free radicals could also force the apoptotic cancer cells' death, meaning that the drug-dependent Ag^+ and ROS release may offer a potent synergistic anticancer activity.

The changes in external/internal stimuli (pH, temperature, redox potential) by releasing drugs into the affected cancer cells can be beneficial in smart drug delivery nanosystems. Ergo, these smart systems can recognize the physiological differences between normal and diseased conditions [8]. Unfortunately, most of the drugs lack a selectivity, resulting in "off-target" and possible cumulative side effects, which limit the therapeutic potential of these highly effective compounds. Furthermore, drug-induced cancer resistance is another obstacle that limits the clinical use of chemotherapeutics [9]. The capture of chemotherapeutics onto biocompatible and biodegradable nanocarriers offers the prospect of minimizing their undesirable toxicity and improves the distribution of active molecules to diseased cells while protecting healthy ones [10].

The monitoring of specific interactions of drugs with biomolecules is one of the important aspects as well. Since the drug undergoes a well-known interaction with DNA, its mechanism may be effectively used for the recognition of damaged and original DNA sequences. Guest molecules for stimuli-responsive nanocarriers, such as chemotherapeutics, can be encapsulated, thus, adsorbed (either electrostatically or chemically) on the nanosubstrate and further released upon altering ambient conditions of cancer cells (as pH, temperature, redox potential). Such systems may help to find much more effective treatment methods than just consuming drugs alone [5]. To minimize non-specific interactions of AgNPs with biomolecules, many stabilizing or capping agents have been used for the AgNPs synthesis as summarized in Table 1. The synthesis of AgNPs is mostly carried out physically (irradiation or temperature gradient) and chemically (reducing agents) [11]. Moreover, biologically mediated synthesis of AgNPs has become of interest due to better biodegradability and biocompatibility of the product, possible reduction of chemical agents need, elimination of an extra step for avoiding AgNPs aggregation, and environmental friendliness. Green synthesis of AgNPs is usually performed using bacteria [12], fungi [13], algae [14], plant extracts [15–18], or amino acids [19].

According to the complexity of drug delivery systems, an appropriate detection mode within existing (bio)analytical methods has to be chosen. To address this issue, electrochemical (bio)sensors as rapid, simple, and inexpensive (bio)

Table 1 The most used stabilizers of AgNPs

Stabilizer	Specification	Ref
Casein	Environmentally friendly polymer to coat, mostly used for antimicrobial activity tests	[20, 21]
Dextrin	Stabilization between reducing ends and longer sugar chains	[20, 22]
Citrate	Stabilization by charge repulsion, weak bonding to the Ag core	[23–28]
Oleate	No significant toxicity to microorganism	[19, 29, 30]
Chitosan	Biocompatible functional molecule with the possibility of further conjunction	[31]
Polyvinylpyrrolidone	Steric stabilization, strong bonding to the Ag core	[20, 23, 25, 26, 32–34]
Polyvinylalcohol	Biocompatible, non-toxic material with antimicrobial properties and optical clarity	[30, 35]
Polyethylene glycol	Steric stabilization, strong bonding to the Ag core	[23, 35]
Polyallylamine hydrochlorid	Adsorbing stabilizer with preferred lower molecular weight	[35]
Polyethylenimine	Non-antimicrobial activity stabilized by positive charge, high stability, blocking of Ag^+ release	[36, 37]

analytical devices could be used to monitor the mechanisms related to AgNPs behavior, their action in drug delivery systems, and to study the interactions of surrounding biomolecules with drugs and their nanocarriers. These sensing tools represent a suitable alternative to other analytical techniques regarding their low cost, undemanding sample treatment, low equipment requirements, fast response, and respectable selectivity and sensitivity to matrix effects. They utilize modern electroanalytical methods that have increasingly been used in the determination of a wide range of biologically active compounds, mainly cancer biomarkers [38]. However, the use of electrochemical sensors in drug delivery design, especially for monitoring a microenvironment-dependent gradual drug release from a nanocarrier, has not widely been applied. Well, considering the advances in nanotechnology, novel sensing (bio)analytical devices have been of interest in order to create cheaper, more practical (bio)sensors with a high level of sensitivity [39]. With a combination of voltammetric and impedimetric approaches, one can obtain complex information about the redox behavior of (bio)molecules of interest as well as the interaction mechanism happening at the electrode-solution interface.

Hereby, we present a comprehensive multi-analytical method-based study of gallic acid-coated AgNPs (GA-AgNPs) of specific size and shape and their undergoing mechanisms that could potentially be used in drug delivery systems for cancer treatment (Fig. 1a). GA-AgNPs were firstly synthesized using gallic acid as a reducing agent. The plasmonic signal of prepared GA-AgNPs was registered spectrophotometrically in the UV–Vis region and an obtained SEM image was used to define their spherical shape and size of approximately 15 nm. The processes related to GA-AgNPs, such as the aggregation and formation of ROS as well as a consecutive Ag^+ release, were monitored by UV–Vis spectral and voltammetric analysis, respectively. Moreover, a complex electrochemical study of the interaction of GA-AgNPs with a low molecular double-stranded DNA (dsDNA) from salmon sperm was performed showing the preferential binding of GA-AgNPs to the sugar-phosphate backbone of dsDNA. This result was also confirmed by FTIR analysis.

Materials and methods

Apparatus

UV–Vis spectral analysis was performed by spectrophotometer Thermo Scientific-Evolution 201 (USA) with 10 mm path quartz cuvettes. FTIR absorption spectra were recorded on Shimadzu IRSpirit FTIR spectrophotometer (Germany) using ATR technique (attenuated total reflectance). Scanning electron microscopy (SEM, JSM-IT500HR, JEOL, Japan) was used to characterize the shape and size of GA-AgNPs. The samples for SEM were prepared on pre-cleaned silicon

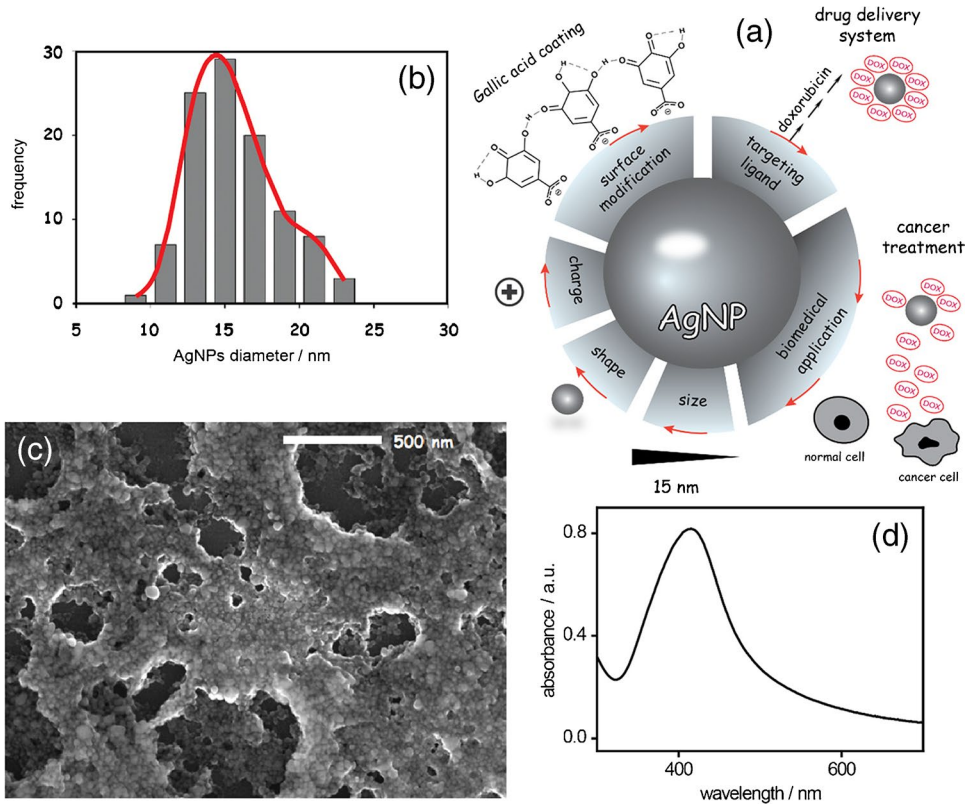

Fig. 1 Characterization of GA-AgNPs: (**a**) schematic illustration of AgNPs characteristics and their application in drug delivery system, (**b**) size distribution diagram, (**c**) SEM image, and (**d**) plasmonic signal at 410 nm

oxide substrates (OSSILA, UK) and processed without prior metal sputtering. During the SEM measurements, an accelerating voltage in the range of 20–25 kV was used. A size distribution diagram was estimated using an image editor ImageJ. Electrochemical measurements as cyclic voltammetry (CV), differential pulse anodic stripping voltammetry (DPASV), differential pulse voltammetry (DPV), and electrochemical impedance spectroscopy (EIS) were performed using the Metrohm Autolab PGSTAT12 Potentiostat/Galvanostat Electrochemical System (Netherlands) driven by the software NOVA version 1.11 (Metrohm Autolab, Netherlands). A three-electrode system composed of a glassy carbon working electrode (GCE) with a disc diameter of 2 mm (Metrohm, Netherlands), a silver/silver chloride reference electrode (Ag/AgCl/sat KCl, L-CHEM, Czech Republic), and a platinum counter electrode was used. Phosphate buffer solution (0.1 mol L^{-1} PB, pH 7.4) was used as a supporting electrolyte. The experiments were performed in 10 mL glass voltammetric cells. For the experiments in UV irradiation, an UV lamp LD 9 W G23 with working wavelength 368 nm was used. All experiments were carried out at ambient temperature. Graphical analysis was performed in software OriginPro 8.0.

Reagents

Salmon sperm dsDNA was purchased from Sigma Aldrich (Slovakia) and its 0.1 mg mL^{-1} stock solution prepared in PB was stored at 4 °C. 4-Chloro-7-nitrobenzofurazan (NBD-Cl) was purchased from Sigma Aldrich (Slovakia) and prepared as a stock solution of 2 mg mL^{-1} (10 mmol L^{-1}) in acetonitrile. GA-AgNPs were synthesized in our laboratory using the protocol described below. Silver nitrate, gallic acid, sodium hydroxide, ammonia, sodium hydrogen phosphate, sodium dihydrogen phosphate, and other required chemicals were obtained from Mikrochem (Slovakia). For GA-AgNPs modification, doxorubicin (DOX) was purchased from Sigma Aldrich (Slovakia) and its 1 mg mL^{-1} stock solution was prepared in deionized water and kept in dark.

GA-AgNPs synthesis and characterization

GA-AgNPs were prepared using a chemical synthesis described by Martínez-Castañon et al. [40]. The reduction of silver ions from silver nitrate took place in the presence of a bioreducing agent, gallic acid, which is known as a phenolic acid naturally occurring in many land plants, fruits, and vegetables. Well, for the synthesis, 16.9 mg of $AgNO_3$ was dissolved in a 100 mL volumetric flask with deionized water and added to a 250 mL beaker. A total amount of 10 mg of GA was dissolved in a 10 mL volumetric flask with deionized water and added to $AgNO_3$ solution under stirring. Afterwards, pH value of the mixture was being adjusted to 10 by a 7.7 mol L^{-1} ammonia solution with the simultaneous generation of spherical GA-AgNPs. The prepared GA-AgNPs were analyzed spectrophotometrically in UV–Vis region from 250 to 900 nm showing a typical narrow absorption band with a maximum at 410 nm (Fig. 1d). The SEM images confirmed a spherical shape of GA-AgNPs (Fig. 1c). A zoomed version of the SEM image (scale of 10 nm) with 102 nanoparticles was used to construct a distribution diagram (Fig. 1b). The average size of GA-AgNPs was automatically calculated using the program ImageJ and was computed to 15 nm. Moreover, the SEM image showed a high degree of GA-AgNPs aggregation.

To modify the silver nanocarriers with DOX, 1 mL of the solution of spherical GA-AgNPs was centrifuged at 10 000 rpm for 10 min. Next, a supernatant was removed and the nanocarrier pellet was dispersed in DOX solution of final concentration 10 µg mL^{-1} in deionized water and allowing it to react for 16 h at controlled temperature 37 °C in dark. The product was centrifuged the next day for 10 min at 10 000 rpm and the supernatant was removed. The functionalized and drug-loaded nanocarriers were washed, dispersed, and centrifuged twice in water. The pellets of GA-AgNPs/DOX nanocarriers were dispersed in 1 mL of desired medium with pH values of 7.0 and 5.5 to mimic the microenvironment of healthy and cancer cells.

Construction of DNA-based biosensor

The GCE surface was first cleaned mechanically by polishing with "alumina slurry" of 0.3 µm (Metrohm, Netherlands) on a mohair paper, washed with nanopure water, and pretreated by applying a potential of + 1.5 V for 300 s in PB under stirring. This anodic pretreatment enhances electrochemical activity over the simply freshly polished electrode surface and the roughness of the electrode surface. At the potential of + 1.5 V, no significant surface changes or topography was found. At higher potentials, the GCE surface can be deactivated due to extensive reduction of the graphite-oxide layer leading to GCE erosion. Zhai et al. confirmed the decreasing of the effective electrode area with growing pretreatment potential, thus, lowering peak currents of analytes accompanied with higher background currents [41]. A voltammetric control scan in 1 mmol L^{-1} redox indicator $[Fe(CN)_6]^{3-/4-}$ was performed to monitor the quality of the bare working electrode. To fabricate the biosensor, a potential-controlled electrostatic deposition of dsDNA from its solution (35 µg mL^{-1}) in PB (pH 7.4) to the GCE surface was applied. Therefore, critical parameters for the preparation of a stable and reproducible DNA layer, such as deposition potential (+ 0.6 V), deposition time (300 s), and scan rate (25 mV s^{-1}), were optimized. An excellent reproducibility of the deposited biolayer was confirmed

by DPV responses of guanine (dGuo) and adenine (dAdo) residues (RSD of 4.66% and 2.15%, respectively). Good stability of the biosensor up to the longest interaction time between dsDNA and GA-AgNPs (60 min) was found and tested by CV measurements of the redox indicator peak current.

Electrochemical analysis

For electrochemical study of the GA-AgNPs interaction with dsDNA, the dsDNA/GCE biosensor was immersed into the aqueous solution of 2-fold diluted GA-AgNPs colloid for up to 60 min. Subsequently, the surface of the biosensor was rinsed with deionized water and electrochemical measurements (CV, EIS, and DPV) were performed under the following conditions: CV in 1 mmol L^{-1} $[Fe(CN)_6]^{3-/4-}$ redox indicator in PB pH 7.4 from − 0.2 to + 0.7 V using the scan rate of 0.1 mV s^{-1} and the step potential of 2 mV; EIS in 1 mmol L^{-1} $[Fe(CN)_6]^{3-/4-}$ using the polarization potential of 0.2 V, the frequency range from 0.1 Hz to 5 kHz (51 frequency steps), and the amplitude of 10 mV. These methods were applied after each step of biosensor modification to control the quality and stability of the prepared biolayer. The interaction between GA-AgNPs present in the solution and dsDNA immobilized at GCE surface was also observed with CV and EIS by monitoring the electron transfer rate and the charge transfer resistance R_{ct} of the working electrode, respectively. Afterwards, the biosensor was rinsed with water and DPV anodic scans in 0.1 M PB pH 7.4 were registered using the scan rate of 25 mV s^{-1}. The DPV peak currents corresponding to the anodic oxidation of dGuo and dAdo were evaluated against the baseline and corrected to the blank.

To confirm the presence of dissolved silver ions and to determine their concentration in GA-AgNPs solutions, the DPASV method was used. The parameters such as conditional potential (+ 1.0 V), potential time (30 s), deposition time (300 s), deposition potential (− 0.3 V), and modulation amplitude (100 mV) using silver nitrate (1 µmol L^{-1}) and sodium nitrate (0.1 mol L^{-1}) as electrolyte were optimized. After the deposition of silver film on the GCE surface, all electrodes were rinsed by deionized water and immersed into pure 0.1 mol L^{-1} sodium nitrate electrolyte. Then, the stripping conditions were applied. For the determination of silver ions, a calibration curve in the concentration range from 0.1 to 1 µmol L^{-1} was obtained. Applying DPASV in various samples (original GA-AgNPs mixture after synthesis, supernatant after centrifugation, and dispersed GA-AgNPs in water after centrifugation), the reoxidation signal of silver ions was investigated and their concentration in each sample was calculated.

Spectral analysis

UV–Vis absorption spectra were obtained within the wavelength range from 300 to 900 nm. For the experiment, quartz crystal cuvettes with a path length of 10 mm were used. Tenfold diluted GA-AgNPs were applied to study the ageing and interaction mechanisms. All experiments were run at room temperature in deionized water, if not specified.

IR spectra with Fourier transformation were recorded in the region from 4000 to 500 cm^{-1} using an ATR diamond crystal. Before each measurement, the crystal was washed with distilled water and acetone, respectively. Then, 5 µL of each aqueous sample was deposited onto the ATR crystal and air-dried to provide an active sampling area by creating a uniform film. Forty-five sample interferograms were acquired at a resolution of 16 cm^{-1}.

Results and discussion

Assessment of aggregation and spontaneous Ag^+ release

To evaluate the quality of the prepared GA-AgNPs, 21-day ageing tests were first performed during which GA-AgNPs were spectrally characterized. Figure 2a (up) shows the UV–Vis absorption spectra of GA-AgNPs taken at various time periods after their exposure to daylight at room temperature. The fresh nanoparticles manifested a sharp and symmetric absorption peak at 410 nm. This well-defined plasmonic peak (surface plasmonic band, SPB) is indicative for relatively large, monodisperse, spherical silver particles. The SPB shape, position, and intensity are strongly dependent on the surrounding medium, size, shape, electronic interactions of the stabilizing ligands with the nanoparticle, and the state of agglomeration which causes red-to-blue visible shifts in absorption spectra [42]. This process starts being observable on the 8th day when a beginning of the tail appearing on the red side of the band can be seen. After 8 days, the absorption band broadens considerably and becomes noticeably asymmetric with the simultaneous formation of the second peak at the red shift. These changes indicate even further aggregation of the particles into clusters in suspension [23, 34]. Moreover, the color of the GA-AgNPs solution changed from yellow to pink (Fig. 2a, down) that confirms the presence of colloidal silver as an initial seed for aggregation [43]. The formation of aggregates can be also seen in SEM image present in Fig. 1c.

DNA-regulated aggregation

For drug delivery systems, the systematically regulated behavior of GA-AgNPs in terms of stability, agglomeration,

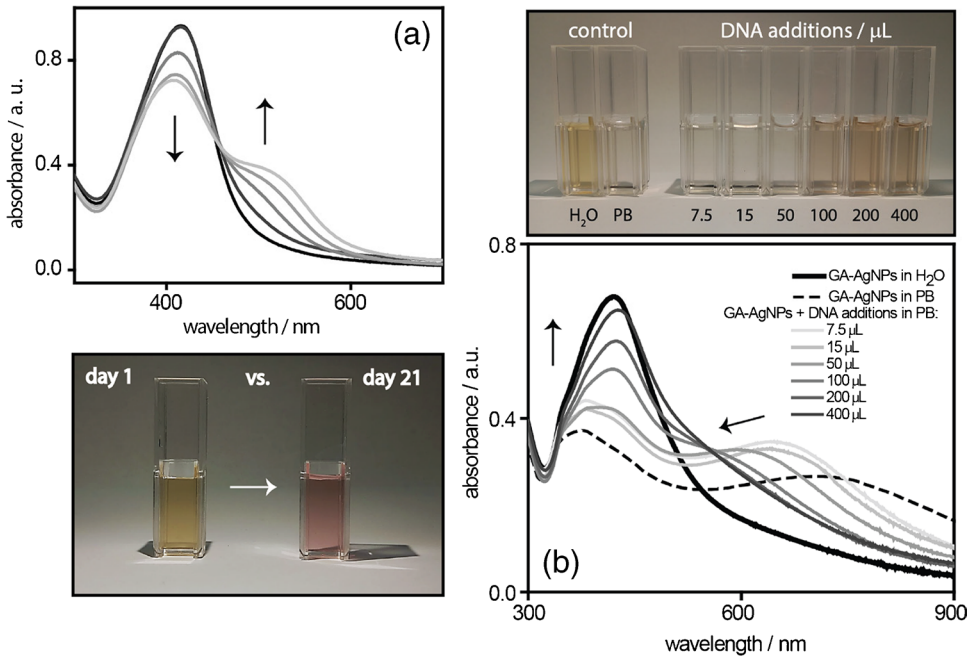

Fig. 2 Spectral and visual analysis of GA-AgNPs aggregation: (**a**) ageing tests showing the aggregation of 16.9 µg mL^{-1} AgNPs using UV–Vis spectral analysis (up) and visual color changes (down), (**b**) dsDNA-regulated aggregation of 16.9 µg mL^{-1} AgNPs in NaCl-free (H_2O) and a phosphate-enriched medium in the absence and presence of various additions of dsDNA using visual (up) and UV–Vis spectral (down) analysis

silver ion releasing, ROS formation, and mutual interactions with ambient biomolecules is required. Especially, the aggregation of nanoparticles serves as a trigger for all these mechanisms and its kinetics depends on particle size, surface charge, and modification with capping agents, the medium chemistry such as the level of dissolved oxygen, pH, ionic strength, electrolyte composition, and the presence of naturally occurred thiol-based organic macromolecules [44, 45]. For the use of nanoparticles as drug nanocarriers, it is necessary to face many challenging conditions in physiological microenvironment. Among them, the presence of monovalent and bivalent ions has been shown to be responsible for the decreased colloidal stability of GA-AgNPs [46]. For this reason, prepared GA-AgNPs were diluted in NaCl-enriched PB solution. Figure 2b (up) demonstrates the visual color changes (from yellow to colorless) of GA-AgNPs colloid diluted in water and PB. To verify the aggregation, UV–Vis absorption spectra of GA-AgNPs were registered (Fig. 2b, down). A well-defined SPB was observed for water-diluted GA-AgNPs, while salt-enriched GA-AgNPs exhibited a significant decrease of the absorption band at 410 nm and a new broad absorption band as an additional red shift was observed (Fig. 2b, down). The stability, regarding the resistance against the salt-induced aggregation, of the prepared nanoparticles was tested in PB in the presence of dsDNA as a potential electrostatic stabilizer. Upon interaction of GA-AgNPs with increasing amount of dsDNA, the SPB at 410 nm became regenerated and narrower as well, thus, it started taking a previous position. DNA molecules obviously served as the stabilizing agents due to the steric stabilization of GA-AgNPs using long-chain dsDNA molecules as well as the charge-based interactions as the electrostatic, van der Waals, and double layer forces between GA-AgNPs aggregates and DNA sugar-phosphate backbone at high level of salt concentration.

Ag^+ release

The conversion of GA-AgNPs into the silver ions as a consequence of their agglomeration was investigated by DPASV. Using a wide range of silver nitrate solution concentrations (Fig. 3a) and the optimized parameters for anodic stripping analysis of silver, the calibration curve was obtained (Fig. 3b). This relation between the reoxidation peak currents and the silver ion content in solution was used for the quantification of released silver in the fresh GA-AgNPs suspension, in the supernatant solution after their centrifugation, and in GA-AgNPs solution after redispersion in water (all samples were 10-fold diluted). The presence of anodic stripping signal of silver at + 0.17 V confirmed the changes of GA-AgNPs accompanied by the aggregation and dissolution to Ag^+ ions. The highest Ag^+ content was found in the supernatant solution after centrifugation (6.97 µmol L^{-1}), while no significant concentration of silver ions in solution after dispersion was observed (1.26 µmol L^{-1}) (Fig. 3c). Comparable results were observed after 1 week in the same samples stored at laboratory temperature and daily light. Here, the determined concentration of silver ions was approximately 1.6–2.6 times higher than in the fresh samples. The time-depending enhanced dissolution of GA-AgNPs under daily light can be expected. These facts

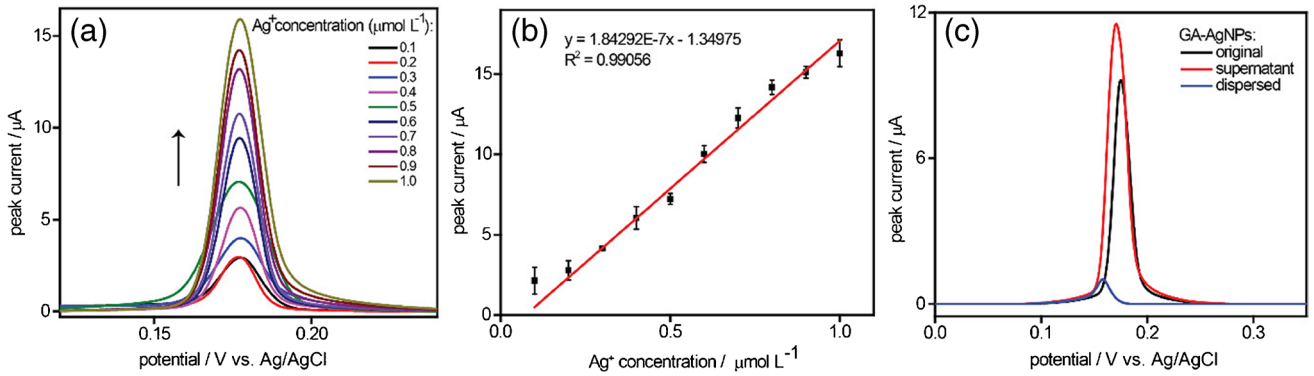

Fig. 3 Determination of silver ions release: (**a**) DPAS voltammograms for various concentrations of silver ions in silver nitrate solution, (**b**) a corresponding calibration curve, and (**c**) DPAS voltammograms for original GA-AgNPs and dispersed after centrifugation

correlate with performed ageing tests at daylight using UV–Vis analysis.

Interaction studies of GA-AgNPs with dsDNA

Electrochemical analysis

The specific interactions of drugs with biomolecules can be used in drug delivery systems, where the drug undergoing a well-known interaction mechanism with DNA may be fixed on a (nano)substrate and this system can be used to recognize a damaged DNA and distinguish it from an original one. Such systems may help to find much more effective treatment methods than just consuming drugs alone. Importantly as well, upon releasing a drug from the AgNPs surface, the positively charged silver aggregates upon releasing silver ions can electrostatically bind to the negatively charged cell membrane and other biomolecules in order to interfere membrane integrity and cause the membrane destabilization and potential DNA damage. Understanding the ensemble of these mechanisms is essential for effectively regulating the (non)wanted effects and consequences of AgNPs reactivity in drug delivery design. For these reasons, electrochemical DNA biosensors may represent promising tools in this field.

Upon exposing DNA to the external physical or chemical agents, such as irradiation or DNA structure-interacting molecules (e.g., drugs), we are able to electrochemically monitor the structural (ir)reversible changes of the biolayer at the electrode surface, either using the electron transfer rate of redox indicators or the direct electrochemistry of DNA nucleobases [47, 48]. Typically, the $[Fe(CN)_6]^{3-/4-}$ complex as a redox indicator is used to test the presence and quality of the DNA layer using CV and EIS. Due to a repulsion between the indicator anions and the negatively charged DNA backbone, a decrease in the CV peak current is observed when compared to that at a bare electrode without DNA [49]. This corresponds well with the results obtained for our dsDNA/GCE biosensor (Fig. 4a). The incubation of the dsDNA/GCE biosensor in GA-AgNPs has caused a further significant decrease of $[Fe(CN)_6]^{3-/4-}$ CV peak current. It indicates an additional barrier effect for the electron transfer between the redox indicator in the solution phase

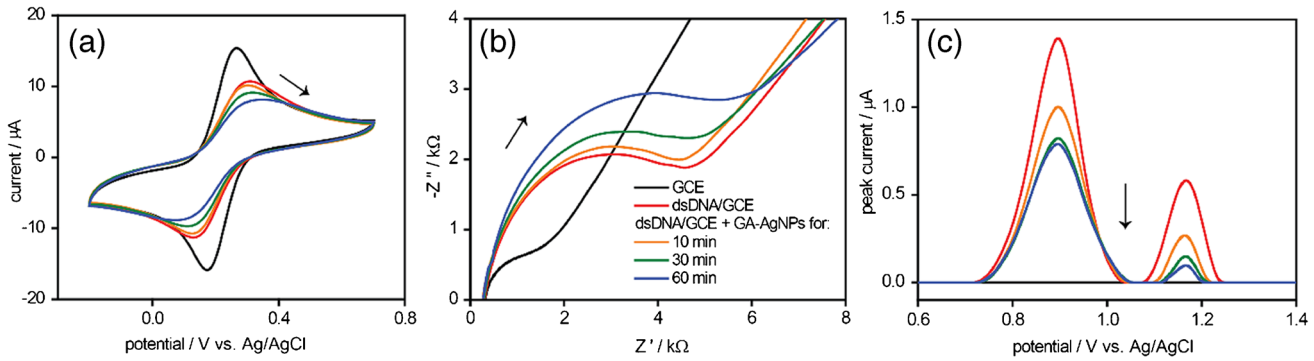

Fig. 4 Electrochemical analysis of the GA-AgNPs-dsDNA interaction using a dsDNA/GCE biosensor: (**a**) cyclic voltammograms and (**b**) Nyquist plots of 1 mmol L^{-1} $[Fe(CN)_6]^{3-/4-}$ as well as (**c**) DP voltammograms of guanine (+0.90 V) and adenine (+1.15 V) residues of dsDNA before and after the exposure of the dsDNA/GCE biosensor to the 16.9 μg mL^{-1} AgNPs colloid for given periods

and the electrode surface evidently caused by a dsDNA-GA-AgNPs association. The probable reason is the formation of the electrostatic interaction between the positively charged silver nanoclusters, that have been confirmed by spectral analysis (Fig. 2a), and the negatively charged DNA phosphate backbone. Within the impedimetric analysis, EIS curves possessed typical Nyquist diagram with the charge transfer resistance values for the electrode surface. Prior to the GA-AgNPs-dsDNA interaction, the DNA layer is characterized by the lowest diameter of the semicircle. With the increasing time of the accumulation, the R_{ct} values gradually increase, which can be observed by increasing the diameter of the semicircle in the Nyquist diagram (Fig. 4b). Thus, the obtained results show a consecutive increase of the charge transfer resistance upon interaction of dsDNA with GA-AgNPs which also indicates a nanoparticle trapping onto the dsDNA structure. These findings correlate with the obtained CV results, where the charge transfer rate is decreasing upon interaction of dsDNA with GA-AgNPs (Fig. 4a).

Moreover, a sensitive DPV technique has been chosen for the investigation of the interaction between dsDNA and GA-AgNPs. Using the direct electrochemistry of nucleic acids, it is possible to principally monitor 2 responses: potential shifting and current changes upon binding guest molecules into the DNA structure. To do so, the dsDNA/GCE biosensor was transferred into PB solution upon the interaction with GA-AgNPs and DP voltammograms were recorded in the positive potential values up to + 1.5 V. The dsDNA/GCE exhibited DPV anodic peaks of deoxyguanosine (dGuo, at + 0.90 V) and deoxyadenosine (dAdo, at + 1.18 V). After the incubation of the biosensor in the GA-AgNPs solution, the peaks of dGuo and dAdo showed a progressive time decrease (Fig. 4c). With a relation to the CV and EIS results, where the changes in charge transfer rate and resistance, respectively, indicated the GA-AgNPs trapping by dsDNA, the silver aggregates then preferentially bind to the DNA phosphate backbone via electrostatic interaction. Therefore, the current signal of dGuo and dAdo consequently decreases, which means the formation of the additional barrier by trapped GA-AgNPs against the nucleobases oxidation. For steric reasons, a direct interaction of dGuo and dAdo inside a double strand with GA-AgNPs is not considered.

FTIR analysis

To deeply investigate the mechanism of the GA-AgNPs-dsDNA interaction, IR analysis accompanied with Fourier transformation was performed using an ATR crystal for a single drop analysis. Before transferring the samples onto the cleaned and dried ATR crystal, they were left on the bench for a few minutes to establish room temperature and to let dsDNA and GA-AgNPs interact together. To verify the results from UV–Vis analysis and electrochemical investigations, FTIR spectra were obtained with dsDNA and GA-AgNPs in concentration range under experimental conditions used for the dsDNA/GCE biosensor. Figure 5 shows the FTIR spectra recorded for dsDNA as well as for the mixture of dsDNA and GA-AgNPs. According to the literature [50], individual absorption bands for dsDNA can be ascribed as follows: 1694 and 1654 cm^{-1} to nucleobases C = O stretching, 1238 cm^{-1} to DNA phosphate asymmetric stretching, 1141 cm^{-1} to DNA phosphate symmetric stretching, 1049 cm^{-1} to C – O *D*-ribose stretching, 913 cm^{-1} to *D*-ribose ring vibration, and 867 cm^{-1} to $C_{3'}$ endo-sugar. After the dsDNA-GA-AgNPs interaction, the absorption bands of nucleobases for the dsDNA–GA-AgNPs mixture were unchanged in the corresponding regions from 1697 to 1655 cm^{-1}. At the same time, the DNA phosphate bands exhibited a shift to higher wavenumbers (1049 to 1061 cm^{-1} and 913 to 964 cm^{-1}). Moreover, the DNA phosphate symmetric stretching at 1141 cm^{-1} disappeared. This all indicated preferential electrostatic interaction of GA-AgNPs with the DNA sugar-phosphate backbone.

GA-AgNPs as perspective drug nanocarriers

Nanoparticles as the particles of ultrasmall size can easily pass through our body system and penetrate through the cell membranes. Hence, they can be used to target the specific disrupted locations of interest. For instance, the passive or active targeting of particular diseased cells or tumor tissues is possible. For this, a combination of mechanisms related to AgNPs, such as aggregation, ion release, ROS formation,

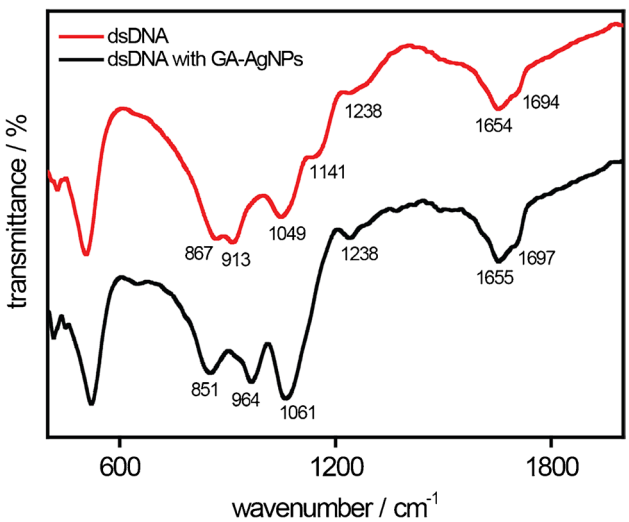

Fig. 5 Spectral analysis of GA-AgNPs and their interaction with dsDNA: FTIR spectra of dsDNA in the absence (red) and presence (black) of GA-AgNPs showing the electrostatic interaction with the DNA phosphate backbone

and a gradual drug release from AgNPs surface, might lead to a potent synergistic therapeutic activity. Since AgNPs have been of interest especially in biomedical applications for their antimicrobial properties, the mechanism behind was found to be attributed to the formation of ROS [4]. That is why the processes related to the AgNPs can be effectively used in targeted drug delivery systems as substrates for drug loading, especially as nanocarriers of chemotherapeutics for cancer treatment and therapy [51].

Detection of ROS formation by NBD-Cl

To test the ROS production by GA-AgNPs, the spectral behavior of the indicator NBD-Cl was exploited since its derivatives have been proved to be extremely useful as a ROS trapping agents [52]. The mixture of 100-fold diluted GA-AgNPs and NBD-Cl (1.5 mL at Petri dish) was exposed to UV-A irradiation for up to 60 min. This irradiation was chosen to study the ROS production in relation to discussed drug delivery system. After each time period, the UV–Vis absorption spectra of NBD-Cl with subtracted spectra of GA-AgNPs (with maximum at 410 nm) were recorded (Fig. 6a). The gradual decrease of the absorbance at 340 nm corresponds to the consecutive oxidation of NBD-Cl. At the same time, the gradual increase of the absorbance at 470 nm can be observed which corresponds to the emerging oxidation peak of NBD-Cl after ROS trapping. The trapping mechanism was also confirmed by an increased absorption band in oxygen-saturated environment (not shown). In the presence of dissolved oxygen, the enhanced aggregation of GA-AgNPs also takes place, compared to GA-AgNPs themselves [27].

pH-sensitive DOX release from GA-AgNPs

The effect of ROS formation in the microenvironment of different pH was studied in order to create the pH-sensitive system for gradual drug release from the GA-AgNPs surface. Since the pH values of normal and cancer cell microenvironment differ (decrease for cancer cells), the physiological (pH 7.0) and weakly acidic (pH 5.5) medium were applied to study the gradual drug release from the nanoparticle surface using the spectral analysis of NBD-Cl. For these purposes, DOX as an oxidative chemotherapeutic agent that can cause a wide range of biological reactions was used. Most importantly, DOX can produce ROS which damage surrounding biomolecules [53]. However, DOX lacks selectivity, resulting in "off-target" and possibly cumulative side effects, which limits its therapeutic potential. The capture of DOX onto the reactive surface of GA-AgNPs could offer the prospect of minimizing undesirable toxicity of DOX for normal cells as well as the ROS-induced damage to cancer cells. Well, DOX-loaded GA-AgNPs were prepared using

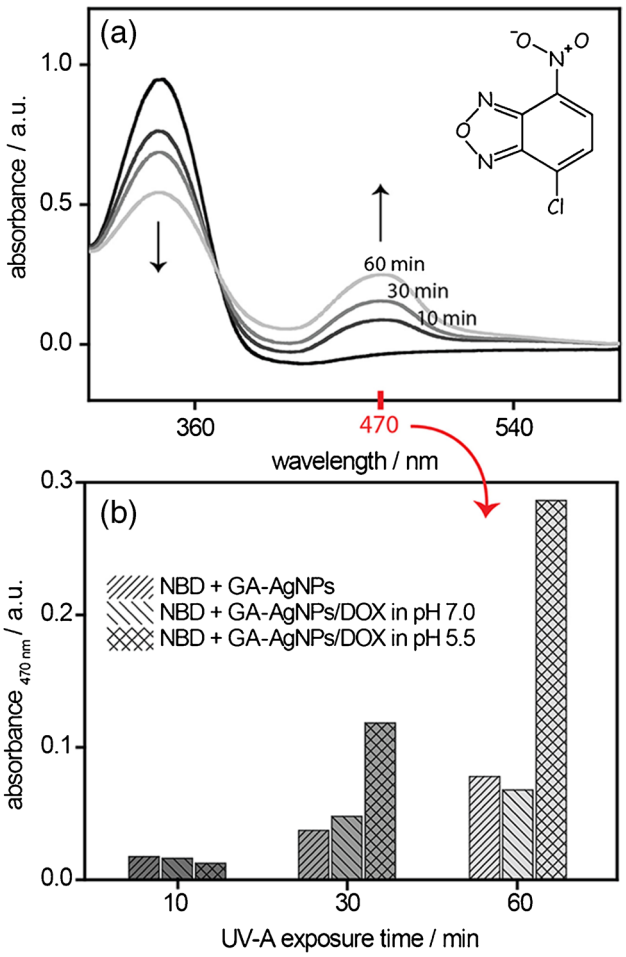

Fig. 6 Drug-loaded GA-AgNPs in physiological and acidic microenvironment: (**a**) UV–Vis absorption spectra of 20.0 μg·mL^{-1} NBD-Cl (340 nm) and its ROS-induced oxidation product (470 nm) in the presence of 16.9 μg·mL^{-1} AgNPs colloid in the UV-A irradiation for given periods, (**b**) evaluation of regulated ROS formation upon DOX loading on GA-AgNPs surface tested in physiological and weakly acidic medium

a protocol described above. Generally, DOX can be easily adsorbed on carboxyl-terminated molecules via hydrogen bonds, van der Waals bonds, or electrostatic interactions [54]. In our case, GA used for the synthesis also serves as the stabilizing agent, thus, creates an organized layer around the nanoparticles [55]. Since GA consists of 3 carboxyl groups in its structure, they can be involved in the immobilization of DOX onto the GA-AgNPs surface as well. Therefore, DOX is fixed onto the GA-AgNPs surface via formation of electrostatic interactions.

The mixture of GA-AgNPs/DOX nanocarriers and NBD-Cl was exposed to the UV-A irradiation at Petri dish for up to 60 min. After each time period, UV–Vis absorption spectra of NBD-Cl with subtracted spectra of GA-AgNPs (with maximum at 410 nm) and DOX (with maximum at 500 nm) were recorded. The gradual decrease of the absorbance

at 340 nm and the gradual increase of the absorbance at 470 nm were again corresponding to the consecutive oxidation of NBD-Cl (Fig. 6b). As shown in the figure, a significantly higher production of ROS (as a consequence of more intensive formation of NBD-Cl oxidation product) was achieved for the GA-AgNPs/DOX complex at pH 5.5 that mimics the pH of endosomes within cancer cells, when compared to their release in pH 7.0. The enhancement of ROS formation is attributed to the synergistic oxidative activity of (a) DOX itself after being detached from the nanosurface and (b) GA-AgNPs themselves after releasing DOX, since both components have been proved to cause the oxidative stress. Lowering of pH from 7.0 to 5.5 led to the gradual DOX release from nanocarriers caused by its weakened interaction with GA-AgNPs at the weakly acidic microenvironment. This was due to the protonation of DOX amino groups, which disrupts hydrogen bonds. Moreover, the loss of a negative charge of carboxyl groups related to GA at the GA-AgNPs surface leads to the DOX detachment from the nanoparticles [56].

The GA-AgNPs/DOX complexes seem to be advantageous for being applied as regulated drug-releasing nanotools, especially with a combination of electrochemical sensor-based detection. Based on the actual results, these complexes have showed a huge potential in drug delivery and that is why DOX-conjugated GA-AgNPs will be of our interest in future studies.

Conclusions and prospects

There is a need for the development of novel strategies to treat cancer, which would ideally target and kill cancer cells selectively as well as would have an improved efficacy/toxicity balance, an enhanced therapeutic index, and an improved pharmacokinetic profile. The ability of nanoparticles to manipulate the (bio)molecules and their structures has revolutionized the conventional drug delivery system. AgNPs, especially those prepared by biosynthesis, offer a valuable tool to novel drug delivery systems in the present scenario because of their biodegradability, biocompatibility, better stability, low toxicity, simple, and mild preparation methods. For these reasons, AgNPs were prepared by the reduction with GA, a natural antioxidant present in many plants and exhibited a wide spectrum of antibacterial activity. The microscopic characterization of GA-AgNPs revealed a spherical shape and a size of 15 nm.

It was found that GA-AgNPs could undergo three major processes in aqueous environments, such as aggregation, dissolution, and ROS generation. In this study, the mechanisms were systematically evaluated using a variety of electrochemical and spectral techniques. To investigate the Ag^+ release, an ageing experiment was performed using UV–Vis spectral analysis. As a result, the aggregation started to take place at 8th day, when a beginning of the tail appeared on the red side of the band was observable. After 8 days, the absorption band became noticeably asymmetric with the simultaneous formation of the second peak at the red shift. Finally, the peak maximum of GA-AgNPs spectra diminished by 24.5%. Using an anodic stripping voltammetry, the highest Ag^+ content was electrochemically determined in the supernatant solution after centrifugation (6.97 $\mu mol \cdot L^{-1}$), while no significant concentration of silver ions in solution after redispersion was observed (1.26 $\mu mol \cdot L^{-1}$). In the presence of dsDNA, the spectrophotometrically tested production of silver aggregates was significantly eliminated which indicated a stabilization effect of long-chain dsDNA on GA-AgNPs.

The interaction of GA-AgNPs present in the solution with dsDNA immobilized at the carbon electrode surface of the biosensor was studied using voltammetric and impedimetric approaches via monitoring the electron transfer rate and the charge transfer resistance of the working electrode, respectively. The results indicated a mutual interaction with the attached dsDNA. The DNA-regulated agglomeration was also proved by DPV applied to the biosensor where the changes in oxidation signals of dGuo and dAdo were studied. The mode of interaction was confirmed by FTIR analysis showing a shift (1049 to 1061 cm^{-1} and 913 to 964 cm^{-1}) specific to DNA phosphate bands. Therefore, the character of the interaction was considered as electrostatic one between the positively charged GA-AgNPs agglomerates and the negatively charged DNA sugar-phosphate backbone.

On the other hand, when GA-AgNPs are used as carriers of anticancer drugs (as doxorubicin, DOX), the ROS formation could be used to enhance the cancer treatment. Previous results demonstrated that GA-AgNPs have possessed high antimicrobial activity against the microbes and relatively lower toxicity towards human healthy cell lines compared to cancer cell lines, which might result from the selective anticancer activity of GA. Furthermore, it was found that GA-AgNPs selectively induced apoptosis in cancer cells [4]. Counting on that, GA-AgNPs were loaded with DOX, and the specific drug release from the GA-AgNPs surface was studied in the physiological and more reactive weakly acidic microenvironment. Since free molecules of DOX are able to produce the oxidation stress to cells, the gradual release of DOX was monitored using a radical scavenger NBD-Cl. The UV–Vis analysis showed a gradual formation of NBD-Cl oxidation product upon mixing with DOX-loaded GA-AgNPs in both, physiological (pH 7.0) and weakly acidic (pH 5.5) microenvironments, where the oxidative effect was significantly higher in pH 5.5 due to the enhanced DOX releasing. DOX can be easily adsorbed on carboxyl-terminated molecules or modified nanoparticles via hydrogen bonds, van der Waals

bonds, or electrostatic interactions. In acidic medium, carboxyl groups lose a negative charge, and the mentioned bonds weaken leading to the release of DOX from the nanoparticle surface. Together, the amino group of DOX is deprotonated in neutral medium and thus allows a hydrogen bond formation. By decreasing pH value, this group becomes protonated and loses an ability to bind to chargeless carboxyl groups. To best of our knowledge, all experimental results correspond well with the theory, while the particular mechanisms associated with GA-AgNPs were in a good agreement with results of other confirming analytical methods. There is still a need to deeply investigate the process of gradual drug release from nanoparticle surfaces in complex matrices, which gives us an initiative to continue working on this problem. Since the aggregation, dissolution, and ROS generation of GA-AgNPs are a function of pH, ionic strength, and electrolyte composition, all of them are key variables to the behavior of GA-AgNPs, both in nature and in engineered environments. It is presumed that the high aggregation grade of GA-AgNPs attenuated their toxic effect on biomacromolecules and living cells. However, the proper coating/capping of AgNPs proved to be less prone to aggregation, thus retaining a degree of their toxicity [46]. Therefore, we will focus on the appropriate stabilizing mechanism of AgNPs colloids via well-selected capping agents (such as polyvinylpyrrolidone or citrate) and on optimizing the concentration ratio between the most suitable capping agent and the loading drug to significantly increase the efficacy of our drug delivery system.

Another future goal is to explore the possibility of using AgNPs in combination with bio-conjugation. The biomolecule-conjugated AgNPs, which have recently been presented as the operable and effective solutions for tedious single nanocarrier-based drug delivery systems, can definitely bring new alternatives to the development of drug delivery systems with higher drug loading capacity. Accordingly, aptamer-coated AgNPs can eventually be utilized as multidrug nanocarriers since aptamers show the high levels of selectivity and specificity.

Acknowledgements This work was supported by the Scientific Grant Agency VEGA of the Slovak Republic (Project No. 1/0159/20). This article was written thanks to the generous support under the Operational Program Integrated Infrastructure for the project: "Strategic research in the field of SMART monitoring, treatment and preventive protection against coronavirus (SARS-CoV-2)," Project no. 313011ASS8, co-financed by the European Regional Development Fund.

Declarations

Conflict of interest The authors declare no competing interests.

References

1. Mandal AK. Silver nanoparticles as drug delivery vehicle against infections. Glob J Nanomedicine. 2017;3(2):555607.
2. Ravindran A, Chandrasekaran N, Mukherjee A. Studies on differential behavior of silver nanoparticles towards thiol containing amino acids. Curr Nanosci. 2012;8(1):141–9 (ISSN 15734137).
3. Agnihotri S, Mukherji S, Mukherji S. Immobilized silver nanoparticles enhance contact killing and show highest efficacy: elucidation of the mechanism of bactericidal action of silver. Nanoscale. 2013;5(16):7328–40 (ISSN 20403372).
4. Li D, Liu Z, Yuan Y, Liu Y, Niu F. Green synthesis of gallic acid-coated silver nanoparticles with high antimicrobial activity and low cytotoxicity to normal cells. Process Biochem. 2015;50(3):357–66 (ISSN 13595113).
5. Hekmat A, Saboury AA, Divsalar A. The effects of silver nanoparticles and doxorubicin combination on DNA structure and its antiproliferative effect against T47D and MCF7 cell lines. J Biomed Nanotechnol. 2012;8(6):968–82 (ISSN 15507033).
6. Pramanik S, Chatterjee S, Saha A, Devi PS, Suresh Kumar G. Unraveling the interaction of silver nanoparticles with mammalian and bacterial DNA. J Phys Chem B. 2016;120(24):5313–24 (ISSN 15205207).
7. Naz M, Nasiri N, Ikram M, Nafees M, Qureshi MZ, Ali S, Tricoli A. Eco-friendly biosynthesis, anticancer drug loading and cytotoxic effect of capped ag-nanoparticles against breast cancer. Appl Nanosci. 2017;7(8):793–802 (ISSN 21905517).
8. Goyal AK, Rath G, Faujdar C, Malik B. Application and perspective of pH-responsive nano drug delivery systems. Elsevier Inc.; 2019.
9. Pushpalatha R, Pharm M, Selvamuthukumar S, Pharm M, Assistant PD, Kilimozhi D, Pharm M, Assistant PD. Nanocarrier mediated combination drug delivery for chemotherapy—a review. J Drug Deliv Sci Technol. 2017;39:362–71 (ISSN 1773-2247).
10 Dong P, Rakesh KP, Manukumar HM, Mohammed YHE, Karthik CS, Sumathi S, Mallu P, Qin HL. Innovative nano-carriers in anticancer drug delivery—a comprehensive review. Bioorg Chem. 2019;85(August 2018):325–36 (ISSN 10902120).
11 Zhang X-F, Liu Z-G, Shen W, Gurunathan S. Silver nanoparticles: synthesis, characterization, properties, applications, and therapeutic approaches. Int J Mol Sci. 2016;17(9):1534 (ISSN 1422-0067).
12. Dakhil AS. Biosynthesis of silver nanoparticle (AgNPs) using Lactobacillus and their effects on oxidative stress biomarkers in rats. J King Saud Univ - Sci. 2017;29(4):462–7 (ISSN 10183647).
13. Roy S, Sadhukhan R, Ghosh U, Das TK. Interaction studies between biosynthesized silver nanoparticle with calf thymus DNA and cytotoxicity of silver nanoparticles. Spectrochim Acta - Part A Mol Biomol Spectrosc. 2015;141:176–84 (ISSN 13861425).
14. El-Naggar NEA, Hussein MH, Shaaban-Dessuuki SA, Dalal SR. Production, extraction and characterization of Chlorella vulgaris soluble polysaccharides and their applications in AgNPs biosynthesis and biostimulation of plant growth. Sci Rep. 2020;10(1):1–19 (ISSN 20452322).
15. Niraimathi KL, Sudha V, Lavanya R, Brindha P. Biosynthesis of silver nanoparticles using Alternanthera sessilis (Linn.) extract and their antimicrobial, antioxidant activities. Colloids Surfaces B Biointerfaces. 2013;102:288–91 (ISSN 09277765).
16. Saravanakumar A, Ganesh M, Jayaprakash J, Jang HT. Biosynthesis of silver nanoparticles using Cassia tora leaf extract and its antioxidant and antibacterial activities. In J Ind Eng Chem. 2015;28:277–81 (ISSN 22345957).
17. Kokila T, Ramesh PS, Geetha D. Biosynthesis of AgNPs using Carica Papaya peel extract and evaluation of its antioxidant and antimicrobial activities. Ecotoxicol Environ Saf. 2016;134:467–73 (ISSN 10902414).

18. KarimiZarchi AA, Mokhtari N, Arfan M, Rehman T, Ali M, Amini M, FaridiMajidi R, Shahverdi ARA. sunlight-induced method for rapid biosynthesis of silver nanoparticles using an Andrachnea chordifolia ethanol extract. Appl Phys A Mater Sci Process. 2011;103(2):349–53 (ISSN 09478396).
19. Suresh AK, Pelletier DA, Wang W, Moon JW, Gu B, Mortensen NP, Allison DP, Joy DC, Phelps TJ, Doktycz MJ. Silver nanocrystallites: biofabrication using shewanella oneidensis, and an evaluation of their comparative toxicity on gram-negative and gram-positive bacteria. Environ Sci Technol. 2010;44(13):5210–5 (ISSN 0013936X).
20. Zhang H, Smith JA, Oyanedel-Craver V. The effect of natural water conditions on the anti-bacterial performance and stability of silver nanoparticles capped with different polymers. Water Res. 2012;46(3):691–9 (ISSN 18792448).
21 Zhong H. Physicochemical properties of protein-modified silver nanoparticles in seawater. Int Nano Lett. 2013;3(1):3–7 (ISSN 2008-9295).
22. Konował E, Sybis M, Modrzejewska-Sikorska A, Milczarek G. Synthesis of dextrin-stabilized colloidal silver nanoparticles and their application as modifiers of cement mortar. Int J Biol Macromol. 2017;104:165–72 (ISSN 18790003).
23. Tejamaya M, Römer I, Merrifield RC, Lead JR. Stability of citrate, PVP, and PEG coated silver nanoparticles in ecotoxicology media. Environ Sci Technol. 2012;46(13):7011–7 (ISSN 0013936X).
24. Zhang W, Yao Y, Sullivan N, Chen Y. Modeling the primary size effects of citrate-coated silver nanoparticles on their ion release kinetics. Environ Sci Technol. 2011;45(10):4422–8 (ISSN 0013936X).
25. Huynh KA, Chen KL. Aggregation kinetics of citrate and polyvinylpyrrolidone coated silver nanoparticles in monovalent and divalent electrolyte solutions. Environ Sci Technol. 2011;45(13):5564–71 (ISSN 0013936X).
26 Li Y, Zhang W, Niu J, Chen Y. Surface-coating-dependent dissolution, aggregation, and reactive oxygen species (ROS) generation of silver nanoparticles under different irradiation conditions. Environ Sci Technol. 2013;47(18):10293–301 (ISSN 0013936X).
27. Zhang W, Yao Y, Li K, Huang Y, Chen Y. Influence of dissolved oxygen on aggregation kinetics of citrate-coated silver nanoparticles. Environ Pollut. 2011;159(12):3757–62 (ISSN 02697491).
28 Ivanova OS, Zamborini FP. Size-dependent electrochemical oxidation of silver nanoparticles. J Am Chem Soc. 2010;132(1):70–2 (ISSN 00027863).
29 Wang W, Efrima S, Regev O. Directing oleate stabilized nanosized silver colloids into organic phases. Langmuir. 1998;14(3):602–10 (ISSN 07437463).
30. Suresh AK, Pelletier DA, Wang W, Morrell-Falvey JL, Gu B, Doktycz MJ. Cytotoxicity induced by engineered silver nanocrystallites is dependent on surface coatings and cell types. Langmuir. 2012;28(5):2727–35 (ISSN 15205827).
31 Nagpal K, Singh SK, Mishra DN. Chitosan nanoparticles: a promising system in novel drug delivery. Chem Pharm Bull. 2010;58(11):1423–30 (ISSN 00092363).
32. Foldbjerg R, Olesen P, Hougaard M, Dang DA, Hoffmann HJ, Autrup H. PVP-coated silver nanoparticles and silver ions induce reactive oxygen species, apoptosis and necrosis in THP-1 monocytes. Toxicol Lett. 2009;190(2):156–62 (ISSN 03784274).
33. Wang H, Qiao X, Chen J, Wang X, Ding S. Mechanisms of PVP in the preparation of silver nanoparticles. Mater Chem Phys. 2005;94(2–3):449–53 (ISSN 02540584).
34. Kvítek L, Panáček A, Soukupová J, Kolář M, Večeřová R, Prucek R, Holecová M, Zbořil R. Effect of surfactants and polymers on stability and antibacterial activity of silver nanoparticles (NPs). J Phys Chem C. 2008;112(15):5825–34 (ISSN 19327447).
35 Radziuk D, Skirtach A, Sukhorukov G, Shchukin D, Möhwald H. Stabilization of silver nanoparticles by polyelectrolytes and polyethylene glycol. Macromol Rapid Commun. 2007;28(7):848–55 (ISSN 10221336).
36 El Badawy AM, Scheckel KG, Suidan M, Tolaymat T. The impact of stabilization mechanism on the aggregation kinetics of silver nanoparticles. Sci Total Environ. 2012;429:325–31 (ISSN 00489697).
37. Batista CCS, Albuquerque LJC, De Araujo I, Albuquerque BL, Da Silva FD, Giacomelli FC. Antimicrobial activity of nano-sized silver colloids stabilized by nitrogen-containing polymers: the key influence of the polymer capping. RSC Adv. 2018;8(20):10873–82 (ISSN 20462069).
38 Cui F, Zhou Z, Zhou HS. Review—measurement and analysis of cancer biomarkers based on electrochemical biosensors. J Electrochem Soc. 2020;167(3):037525 (ISSN 0013-4651).
39. Ghalkhani M, Kaya SI, Bakirhan NK, Ozkan Y, Ozkan SA. Application of nanomaterials in development of electrochemical sensors and drug delivery systems for anticancer drugs and cancer biomarkers. Crit Rev Anal Chem. 2020;1–23. https://doi.org/10.1080/10408347.2020.1808442.
40. Martinez-Castanon GA, Niño-Martínez N, Martínez-Gutierrez F, Martínez-Mendoza JR, Ruiz F. Synthesis and antibacterial activity of silver nanoparticles with different sizes. J Nanoparticle Res. 2008;10(8):1343–8 (ISSN 13880764).
41 Zhai H, Wang S, Zhou J, Pan J, Tong Y, Mei Q, Zhou Q. A simple and sensitive electrochemical sensor for 3-nitrotyrosine based on electrochemically anodic pretreated glassy carbon electrode in anionic surfactant medium. J Electrochem Soc. 2019;166(15):B1426–33 (ISSN 0013-4651).
42. Štruncová M, Toma SH, Araki K, Bresciani E, Rodrigues FP, Medeiros IS, Dutra-Correa M. Silver nanoparticles added to a commercial adhesive primer: colour change and resin colour stability with ageing. Int J Adhes Adhes. 2020;102:102694 (ISSN 01437496).
43 Solomon SD, Bahadory M, Jeyarajasingam AV, Rutkowsky SA, Boritz C, Mulfinger L. Synthesis and study of silver nanoparticles. J Chem Educ. 2007;84(2):322–5 (ISSN 00219584).
44. Baalousha M, Nur Y, Römer I, Tejamaya M, Lead JR. Effect of monovalent and divalent cations, anions and fulvic acid on aggregation of citrate-coated silver nanoparticles. Sci Total Environ. 2013;454–455:119–31 (ISSN 00489697).
45. Oukarroum A, Samadani M, Dewez D. Influence of pH on the toxicity of silver nanoparticles in the green alga Chlamydomonas acidophila. Water Air Soil Pollut. 2014;225(8):1–8 (ISSN 15732932).
46 Bélteky P, Rónavári A, Igaz N, Szerencsés B, Tóth IY, Pfeiffer I, Kiricsi M, Kónya Z. Silver nanoparticles: aggregation behavior in biorelevant conditions and its impact on biological activity. Int J Nanomedicine. 2019;14:667–87 (ISSN 11782013).
47. Svitkova V, Blaskovicova J, Tekelova M, Kallai BM, Ignat T, Horackova V, Skladal P, Kopel P, Adam V, Farkasova D, Labuda J. Assessment of CdS quantum dots effect on UV damage to DNA using a DNA/quantum dots structured electrochemical biosensor and DNA biosensing in solution. Sensors Actuators, B Chem. 2017;243:435–44 (ISSN 09254005).
48 Nemčeková K, Labuda J, Milata V, Blaškovičová J, Sochr J. Interaction of DNA and mononucleotides with theophylline investigated using electrochemical biosensors and biosensing. Bioelectrochemistry. 2018;123:182–9 (ISSN 1878562X).
49 Labuda J, Brett AMO, Evtugyn G, Fojta M, Mascini M, Ozsoz M, Palchetti I, Paleček E, Wang J. Electrochemical nucleic acid-based biosensors: concepts, terms, and methodology (IUPAC Technical Report). Pure Appl Chem. 2010;82(5):1161–87 (ISSN 0033-4545).
50. Serec K, Šegedin N, Krajačić M, Babić SD. Conformational transitions of double-stranded dna in thin films. Appl Sci. 2021;11(5):1–18 (ISSN 20763417).

51. Ramalingam V, Varunkumar K, Ravikumar V, Rajaram R. Target delivery of doxorubicin tethered with PVP stabilized gold nanoparticles for effective treatment of lung cancer. Sci Rep. 2018;8(1):1–12 (ISSN 20452322).
52 Olojo RO, Xia RH, Abramson JJ. Spectrophotometric and fluorometric assay of superoxide ion using 4-chloro-7-nitrobenzo-2-oxa-1,3-diazole. Anal Biochem. 2005;339(2):338–44 (ISSN 00032697).
53 Tacar O, Sriamornsak P, Dass CR. Doxorubicin: an update on anticancer molecular action, toxicity and novel drug delivery systems. J Pharm Pharmacol. 2013;65(2):157–70 (ISSN 00223573).
54 Patra S, Mukherjee S, Barui AK, Ganguly A, Sreedhar B, Patra CR. Green synthesis, characterization of gold and silver nanoparticles and their potential application for cancer therapeutics. Mater Sci Eng C. 2015;53:298–309 (ISSN 09284931).
55. Farrokhnia M, Karimi S, Askarian S. Strong hydrogen bonding of gallic acid during synthesis of an efficient AgNPs colorimetric sensor for melamine detection via dis-synthesis strategy. ACS Sustain Chem Eng. 2019;7(7):6672–84 (ISSN 21680485).
56 Maleki R, Afrouzi HH, Hosseini M, Toghraie D, Piranfar A, Rostami S. pH-sensitive loading/releasing of doxorubicin using single-walled carbon nanotube and multi-walled carbon nanotube: a molecular dynamics study. Comput Methods Programs Biomed. 2020;186:105210 (ISSN 18727565).